

# Ideal Strength of Doped Graphene

S. J. Woo and Young-Woo Son\*

*Korea Institute for Advanced Study, Seoul 130-722, Korea*

(Dated: May 24, 2022)

While the mechanical distortions change the electronic properties of graphene significantly, the effects of electronic manipulation on its mechanical properties have not been known. Using first-principles calculation methods, we show that, when graphene expands isotropically under equibiaxial strain, both the electron and hole doping can maintain or improve its ideal strength slightly and enhance the critical breaking strain dramatically. Contrary to the isotropic expansions, the electron doping decreases the ideal strength as well as critical strain of uniaxially strained graphene while the hole doping increases both. Distinct failure mechanisms depending on type of strains are shown to be origins of the different doping induced mechanical stabilities. Our findings may resolve a contradiction between recent experimental and theoretical results on the strength of graphene.

PACS numbers: 62.20.-x, 63.20.kd, 63.22.Rc, 81.40.Jj

## I. INTRODUCTION

A defect-free infinite crystal becomes mechanically unstable at a stress with a corresponding critical strain. Such a stress is the ideal strength of a material which is an inherent property of a given atomic and electronic structure as well as a natural upper bound on its strength<sup>1,2</sup>. While the variation of electron density can alter ideal strength of some materials<sup>3</sup>, those manipulations usually involve stoichiometric change which may alter the nature of chemical bonding between atoms in crystal. In this regard, graphene, a two-dimensional crystal with atomic thickness, is an ideal material to investigate electronic control of ideal strength because it allows very high level of charge doping without any sacrifice of atomic integrity through either field-effect transistor setups<sup>4,5</sup> or alkali metal depositions<sup>6</sup>. Although there have been many studies about effects of mechanical perturbation on electron physics in graphene<sup>7-12</sup>, the effect of electron density variation on the mechanical properties of graphene has not been known yet.

Graphene is also known to be the strongest two dimensional (2D) material<sup>13</sup> and can maintain its strength in the presence of grain boundaries<sup>14</sup>. A recent nanoindentation experiment<sup>13</sup> reports that the intrinsic strength of graphene is  $42 \text{ N m}^{-1}$  at the nominal equibiaxial breaking strain of 0.225. This was followed by a theoretical calculation<sup>15</sup> showing the quite smaller breaking strain of 0.15 than the measured value. It is unusual since materials under strain typically fail before they reach the ideal strength due to various reasons. Therefore considerations on the other external effects such as a doping are called for to understand the ideal strength of graphene further since typical graphene samples in experiments are doped.

In this work, we report a theoretical study showing that graphene under equibiaxial strain becomes to be stronger as doping increases with both electron and hole doping. Though the ideal strength under equibiaxial strain increases slightly by  $1 \sim 6 \%$  depending on doping type and amounts, the corresponding critical break-

ing strain increases dramatically by  $\sim 19 \%$  within the doping level of  $\sim 1.1 \times 10^{14} / \text{cm}^2$  which is accessible in experiments<sup>5,6</sup>. We show that the failure of isotropically expanded graphene through the  $A'_1$  phonon mode softening<sup>15</sup> or the two-dimensional Peierls instability<sup>16</sup> is overcome by doping because the Fermi level ( $E_F$ ) of doped graphene lies outside the energy gap associated with the  $A'_1$  phonon. On the contrary, under uniaxial strain invoking elastic failure of graphene<sup>15</sup>, we find that electron doping weakens graphene by  $5 \sim 7 \%$  while hole doping strengthens one by  $3 \sim 6 \%$  and that the corresponding breaking strains also change a lot by  $37 \%$  within similar doping levels for the equibiaxial strain cases. Because the elastic failure under uniaxial strain is associated with occupation of the  $\sigma^*$  band<sup>10</sup>, the asymmetric dependence of ideal strength on electron and hole doping can be explained in term of doping induced occupation (electron doping) or depopulation (hole doping) of the  $\sigma^*$  band of uniaxially strained graphene.

This paper is organized as follows. In Sec. II, we introduce calculation methods used in this work. After introducing models for the first-principles calculations, we examine the ideal strength of graphene under equibiaxial strains with various electron and hole dopings in Sec. III. Then, we also study the ideal strength of doped graphene under uniaxial strain with different strain directions and reveal origins of variations in ideal strength depends on strain as well as dopings in Sec. IV. In Sec. V, we discuss a possible resolution on discrepancy between experiment<sup>13</sup> and theoretical works<sup>15,16</sup> and conclude this work.

## II. CALCULATION METHODS

Our first-principles calculations<sup>17</sup> are carried out with plane wave basis and norm-conserving pseudopotentials<sup>18</sup>. The local density approximation (LDA) is used for the exchange-correlation functional<sup>19</sup>. Phonon spectrum is calculated using density functional perturbation theory<sup>17,20</sup> with  $12 \times 12 \times 1$   $q$ -point sampling. The energy cutoff for the basis set expansion is 80 Ry. The

$k$ -point grid of  $48 \times 48 \times 1$  is used. Doping is simulated within the rigid band approximation which is successfully used in recent studies on Kohn anomaly of doped carbon nanotubes<sup>21</sup> and graphene<sup>22</sup> respectively. Near the Kohn anomaly where the phonon frequency changes very abruptly in a narrow momentum range, the explicit phonon calculations are additionally done to avoid the inherent errors in interpolated phonon dispersions.

### III. IDEAL STRENGTH OF DOPED GRAPHENE UNDER EQUIBIAXIAL STRAIN

When graphene expands isotropically, the  $A'_1$  phonon mode at the  $K$  point softens and then becomes to be unstable at a certain critical equibiaxial strain<sup>15</sup>. The inset of Fig. 1 (a) show schematically how the crystal structure of graphene is deformed when the  $A'_1$  phonon is excited. Here, the strain is defined by  $\epsilon = (a - a_0)/a_0$ , where  $a$  and  $a_0$  are the lattice constant of equibiaxially strained graphene and that of pristine graphene respectively. In Fig. 1 (a), the total energy variations as a function of the amplitude of  $A'_1$  phonon mode show that, for  $\epsilon > 0.15$ , the hexagonally deformed structure is energetically more stable than the symmetric one<sup>15</sup>. For these calculations we use the  $K$ -point supercell in which six carbon atoms are included [inset of Fig. 1(a)]<sup>15</sup>. This can be understood as two-dimensional extension of Peierls instability<sup>16</sup>. Undoped graphene has its  $E_F$  at the Dirac point and the excitation of  $A'_1$  phonon mode generates a dynamical energy gap at the point<sup>16,23</sup> realizing the Kohn anomaly<sup>23,24</sup>. As graphene expands over critical equibiaxial strain, the energy gain through formation of static energy gap at the  $K$ -point overcomes the energy cost for ion-ion interaction so that the hexagonal network of graphene breakdowns<sup>15,16</sup>. Therefore, if the  $E_F$  shifts away from the Dirac point by doping, the Peierls instability will be avoided by hardening the  $A'_1$  phonon so that graphene becomes more resistive against the applied equibiaxial strain.

To confirm this hypothesis, we calculate the total energy of doped graphene when the  $A'_1$  phonon mode is excited. As discussed, Fig. 1 (a) shows the lattice instability of undoped graphene over a critical equibiaxial strain ( $\epsilon > 0.15$ ). The same calculations were performed for doped graphene at various doping levels with a fixed overcritical strain of  $\epsilon = 0.16$  [Figs. 1 (b) and (c)]. The electron (hole) doping level,  $n_e(n_h)$ , is defined by the number of additional electrons (holes) per a carbon atom. We note that  $n_e = 0.01$  corresponds to  $3.848 \times 10^{13}$  electron/cm<sup>2</sup>. As shown in Figs. 1 (b) and (c), the electron and hole dopings indeed recover the stability of  $A'_1$  phonon mode even at the strain of  $\epsilon = 0.16$  under which pristine graphene is already broken.

To obtain complete ideal strengths ( $\sigma_{\text{ideal}}$ ) of doped graphene, the stress-strain relationships are needed, in which the maximum stress at the critical strain ( $\epsilon_{\text{critical}}$ ) is the  $\sigma_{\text{ideal}}$  of doped graphene. In Figs. 2 (a) and (b),

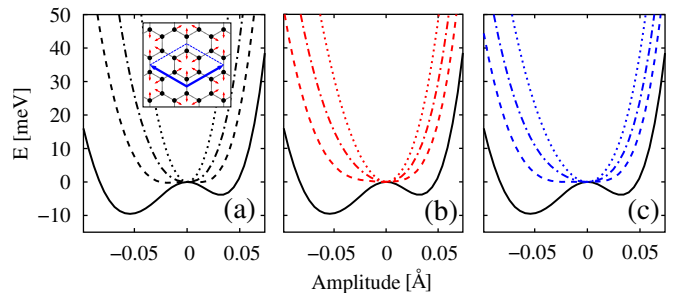


FIG. 1: (Color online) (a) The total energy variation as a function of  $A'_1$  phonon amplitude under equibiaxial strains of  $\epsilon = 0.12, 0.14, 0.15$ , and  $0.16$  from top to bottom lines. Inset shows schematic atomic displacements (red arrows) of the  $A'_1$  phonon mode and the  $K$ -point supercell (blue arrows). (b) and (c) show the same curves as in (a) at a fixed strain,  $\epsilon = 0.16$ , with changing electron and hole doping from top to bottom lines,  $n_e(n_h) = 0.04, 0.02, 0.01, 0.0$  respectively.

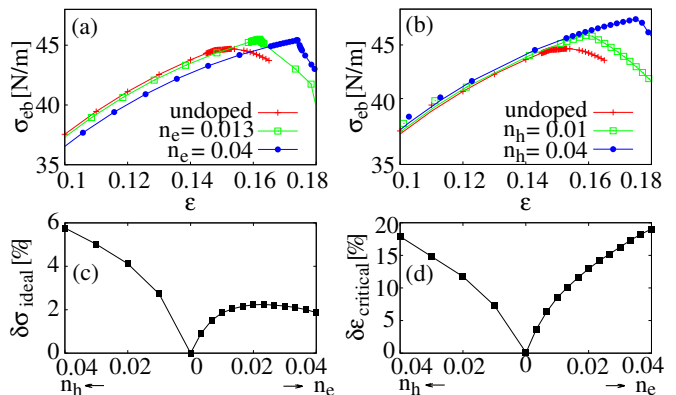


FIG. 2: (Color online) (a) and (b) show the stress-strain relationship of graphene under equibiaxial strains with different electron and hole doping levels respectively. The equibiaxial strain is defined by  $\sigma_{\text{eb}} \equiv \sqrt{\sigma_x^2 + \sigma_y^2}/\sqrt{2}$ . The variations (in percentage) of (c) ideal strength ( $\delta\sigma_{\text{ideal}}$ ) and (d) corresponding critical breaking strain ( $\delta\epsilon_{\text{critical}}$ ) of doped graphene with respect to those of undoped one as a function of doping.

stress maximum in the stress-strain relationship of doped graphene shifts toward larger strain as the doping increases independent of the doping type. The  $\sigma_{\text{ideal}}$  of undoped graphene is  $44.6$  N/m agreeing well with recent studies<sup>13,15</sup>. The critical breaking strain of  $0.148$ , however, is much smaller than the measured value<sup>13,15,16</sup>. As  $n_e$  increases from  $0.00$  to  $0.04$ ,  $\sigma_{\text{ideal}}$  increases by  $\sim 2\%$  ( $n_e = 0.02$ ) and then decreases. As  $n_h$  increases from  $0.00$  to  $0.04$ ,  $\sigma_{\text{ideal}}$  increases monotonically by  $\sim 6\%$  [Fig. 2(c)]. Contrary to that, the  $\epsilon_{\text{critical}}$  shows a dramatic increase by  $\sim 19\%$  ( $\epsilon_{\text{critical}} \sim 0.19$ ) as both  $n_e$  and  $n_h$  increase to  $0.04$  [Fig. 2(d)].

We have further calculated phonon dispersions in order to see how the phonon softening at the  $K$ -point is affected by the doping. Softening of phonon to the negative phonon frequency may precede or indicate the crystal instability<sup>25</sup>. Fig. 3 (a) shows the phonon dispersion of

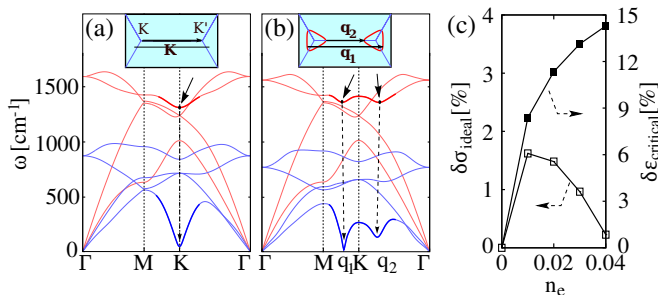


FIG. 3: (Color online) (a) Phonon dispersion of undoped graphene with equibiaxial strain  $\epsilon = 0$  (red lines) and 0.148 (blue). (b) Same as in (a) except for doped graphene ( $n_e = 0.04$ ) with  $\epsilon = 0$  (red) and 0.167 (blue). In both panels, the black arrows indicate the Kohn anomaly and the insets show the vectors (black arrows) connecting Fermi surfaces (red lines) related with the Kohn anomaly. Here we do not show irrelevant out-of-plane phonon mode spectrum. (c)  $\delta\sigma_{\text{ideal}}$  and  $\delta\epsilon_{\text{critical}}$  (left and right ordiates) obtained from phonon dispersions as function of electron doping  $n_e$  (abscissa).

graphene with  $\epsilon = 0$  (red) and  $\epsilon = 0.148$  (blue) agreeing well with a previous study<sup>15</sup>. The frequency dip at the  $K$ -point associated with the  $A'_1$  mode is the Kohn anomaly<sup>23,24</sup>. We note that the LDA is not quantitatively perfect to describe the anomaly<sup>26</sup> but is sufficient to describe the softening within certain errors<sup>15,21,22</sup>. The Kohn anomaly may occur for a phonon of momenta  $\mathbf{q}$  when two electronic states of momentum  $\mathbf{k}_1$  and  $\mathbf{k}_1 + \mathbf{q}$  are on the Fermi surface<sup>24,27</sup>. In undoped graphene, the Fermi surface is at the Dirac points located at  $\mathbf{K}$  and  $\mathbf{K}' = 2\mathbf{K}$  so that  $\mathbf{q} = 0$  ( $\Gamma$ -point) and  $\mathbf{q} = \mathbf{K}$  ( $K$ -point) are allowed for the anomaly. The inset in Fig. 3 (a) shows the corresponding vector  $\mathbf{K}$  in the BZ. As graphene doped, the momentum at which the anomaly occurs shifts from the  $K$ -point and splits into two points. The  $A'_1$  phonon hardens also because of change of the  $E_F$ . In electron-doped graphene ( $n_e = 0.04$ ), the Kohn anomaly occurs both at  $q_1$  between  $M$  and  $K$  and at  $q_2$  between  $K$  and  $\Gamma$  [Fig. 3 (b)]. The inset in Fig. 3 (b) shows the corresponding vectors  $\mathbf{q}_1$  and  $\mathbf{q}_2$  connecting the two electronic states at Fermi surfaces of two valleys in doped graphene. The phonon at  $q_1$  softens to zero frequency at the critical equibiaxial strain of  $\epsilon = 0.167$  [Fig. 3 (b)]. This indicates that the doped graphene becomes structurally unstable through the less symmetric phonon mode at  $q_1$  than  $A'_1$  mode. The strain value of 0.167 for  $n_e = 0.04$  doping differs from the corresponding critical strain of 0.179 obtained by the stress-strain relationship [Fig. 2 (d)].

By taking stress and strain values when the softened phonon mode touches zero frequency, we can also obtain the doping dependent ideal strengths and the corresponding critical strains. As shown in Fig. 3 (c), the overall behaviors of  $\delta\sigma_{\text{ideal}}$  and  $\delta\epsilon_{\text{critical}}$  are similar to those obtained (Figs. 2 (c) and (d)) from the stress-strain curves. However, the ideal strength increases only by  $\sim 1.7\%$  and then decreases back to the original value as  $n_e$  reaches

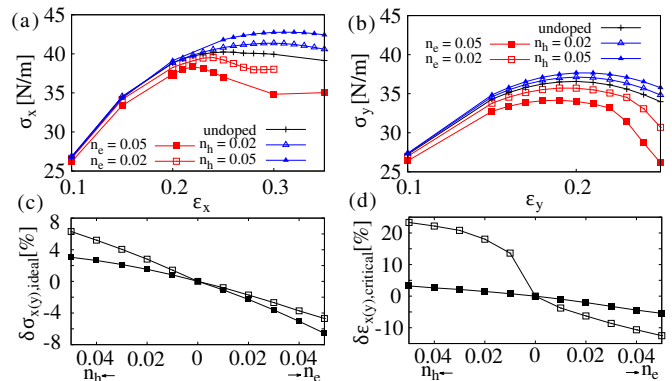


FIG. 4: (Color online) Stress-strain curves for graphene under (a) zigzag ( $\epsilon_x$ ) and (b) armchair ( $\epsilon_y$ ) strain with various doping levels. The variations (in percentage) of (c) ideal strength and (d) critical breaking strain as a function of the doping level for graphene under the  $\epsilon_x$  (open rectangles) and  $\epsilon_y$  (solid ones) respectively.

0.04 [Fig. 3(c)] due to phonon softening at  $q_1$ . The corresponding breaking strain shows the significant increase by  $\sim 15\%$ . So, we can conclude that under equibiaxial strain the electron and hole doping improve the ideal strength slightly or at least maintain its undoped value while the corresponding critical strain increases dramatically by doping. These interesting behaviors of stress and strain of doped graphene can be understood by noting that the ideal strength is mostly determined by  $\sigma$  bonds between carbon atoms that does not be affected much by the doping but that the breaking point of strain is determined by  $\pi$  bands owing to the Kohn anomaly that changes greatly according to the doping.

#### IV. IDEAL STRENGTH OF DOPED GRAPHENE UNDER UNIAXIAL STRAIN

We have analyzed the ideal strength of doped graphene under uniaxial strains. Unlike the equibiaxial strain cases, the uniaxial strain breaks the crystal symmetry of graphene so that Dirac cone moves away from  $K$ -point and distorts into anisotropic form<sup>9,10</sup>. Here we only consider uniaxial strains either along zigzag or armchair direction<sup>9,10</sup> (called as zigzag ( $\epsilon_x$ ) and armchair ( $\epsilon_y$ ) strain respectively) and calculate the stress-strain relationship to find out the doping dependent ideal strength. For these calculations, the primitive unit cell including two carbon atoms is used since uniaxially strained graphene breaks down elastically unlike equibiaxial strain cases<sup>15</sup>. Fig. 4 (a) and (b) show the stress-strain curves for the zigzag and armchair strain respectively with different doping levels. It is found that the ideal strength under zigzag strain is more sensitive on the doping than that under the armchair one. Figs. 4 (c) and (d) show the change of ideal strength and critical strain as function of dopings respectively. Contrary to the equibiaxial strain

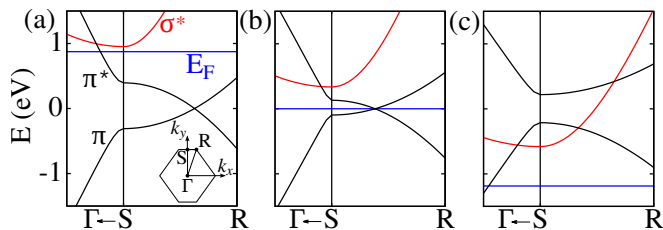


FIG. 5: (Color online) Electronic band structures of graphene under (a) the zigzag strain of  $\epsilon_x = 0.22$  with  $n_e = 0.05$ , (b)  $\epsilon_x = 0.25$  without doping, and (c)  $\epsilon_x = 0.30$  with  $n_h = 0.05$ . The red and black lines are the  $\sigma^*$  and  $\pi(\pi^*)$  bands respectively and the blue is the Fermi level. The inset in (a) shows the high symmetry points of BZ of graphene with  $\epsilon_x$ .

case, the response of graphene under uniaxial strain is asymmetric with respect to the electron and hole doping: graphene becomes stronger with the hole doping while it becomes weaker under the electron doping. For undoped graphene, the maximum stress of  $\sigma_{\text{ideal}} = 40.2$  (36.6) occurs at  $\epsilon_{\text{critical}} = 0.253$  (0.198) for the zigzag (armchair strain) agreeing with a previous study<sup>28</sup>. Similar to the equibiaxial strain case, the doping induce a huge change of the strain values but not the ideal strength [Figs. 4(c) and (d)]. Under zigzag strain, the critical breaking strain increases from 0.253 to 0.311 (23% increase) as  $n_h$  reaches 0.05, and decreases to 0.22 (13% decrease) as  $n_e$  reaches 0.05. On the other hand, under the armchair strain, it increases only by 3.5% and decreases by 5% in the same condition.

Especially under the zigzag strain, the two Dirac cones at the  $K$ - and  $K'$ -point approach each other and eventually merge after a critical strain opening a small energy gap at the merged point<sup>9,10,29</sup>. At the same time, however, the energy of  $\sigma^*$  band is lowered toward the  $E_F$ <sup>10</sup> signaling the breakdown of crystal structure. Our calculation shows that the stress maximum occurs as the unoccupied  $\sigma^*$  band reaches the  $E_F$ . Figs. 5 (a), (b) and (c) show the electronic band structure for electron-doped, undoped, and hole-doped graphene under the zigzag strain respectively. For the electron doping with  $n_e = 0.05$  the  $\sigma^*$  band is closer to the  $E_F$  compared with one in undoped graphene under zigzag strain so that the

band is filled up at a relatively lower strain of  $\epsilon_x = 0.22$  [Fig. 5 (b)]. Contrary to that, for the hole doping with  $n_h = 0.05$  the  $\sigma^*$  band moves away from the  $E_F$  so that it requires relatively higher strain of  $\epsilon_x = 0.30$  for the band to be filled up [Fig. 5 (c)]. This explains the physical origin of electron-hole doping asymmetry of the ideal strength of doped graphene under zigzag strain.

## V. DISCUSSION AND CONCLUSION

We discuss a possible resolution of the discrepancy between the recent experiment<sup>13</sup> and theories<sup>15,16</sup> on the strength of graphene. From our calculations, the doped graphene can exhibit a theoretical ideal strength ( $> 40$  N m<sup>-1</sup>) with a enhanced critical equibiaxial strain. Though the amount of doping in the experiment<sup>13</sup> has not been known, the combination of several unknown experiment factors such as anisotropy in applied forces<sup>13</sup>, formation of dislocation<sup>14</sup>, and non-uniformity in number of layers as well as doping may enhance the critical strain value further than the undoped maximum of  $\epsilon = 0.148$ .

In conclusion, we show that the doping induces significant strain-dependent variations in the mechanical stability of graphene. Thus, our calculations set new bounds on the ideal strength and critical strain of graphene in realistic situations. We believe that our study not only highlights interesting interplay between electronic and mechanical properties of graphene but also will be useful to explore such properties in other 2D crystals<sup>30</sup>.

*Note added.* After submission, we became aware of a recent paper<sup>31</sup> having an overlap with a part of our work which was also reported recently<sup>32</sup>.

## Acknowledgments

This work is supported by the NRF of Korea grant funded by MEST (QMMRC, No. R11-2008-053-01002-0 and CASE, No. 2011-0031640). Computations are supported by KISTI Supercomputing Center (Project No. KSC-2011-C1-21) and the CAC of KIAS.

\* Electronic address: hand@kias.re.kr

<sup>1</sup> A. Kelly and N. H. Macmillan, *Strong Solids* (Clarendon, Oxford, 1986).

<sup>2</sup> J. W. Moriss, Jr., C. R. Krenn, D. Roundy, and M. L. Cohen, in *Phase Transformation and Evolution in Materials*, edited by P. E. A. Turchi and A. Gonis (The Minerals, Metals and Materials Society, Warrendale, PA, 2000).

<sup>3</sup> S.-H. Jhi, J. Ihm, S. G. Louie, and M. L. Cohen, *Nature* **399**, 132 (1999).

<sup>4</sup> K. S. Novoselov, A. K. Geim, S. V. Morozov, D. Jiang, Y. Zhang, S. V. Dubonos, I. V. Grigorieva, and A. A. Firsov, *Science* **306**, 666 (2004).

<sup>5</sup> D. K. Efetov and P. Kim, *Phys. Rev. Lett.* **105**, 256805 (2010).

<sup>6</sup> J. L. McChesney, A. Bostwick, T. Ohta, T. Seyller, K. Horn, J. González, and E. Rotenberg, *Phys. Rev. Lett.* **104**, 136803 (2010).

<sup>7</sup> F. Guinea, M. I. Katsnelson, and A. K. Geim, *Nat. Phys.* **6**, 30 (2009).

<sup>8</sup> V. M. Pereira and A. H. Castro Neto, *Phys. Rev. Lett.* **103**, 046801 (2009).

<sup>9</sup> V. M. Pereira, A. H. Castro Neto, and N. M. R. Peres, *Phys. Rev. B* **80**, 045401 (2009).

<sup>10</sup> S.-M. Choi, S.-H. Jhi, and Y.-W. Son, *Phys. Rev. B* **81**,

- 081407 (2010).
- <sup>11</sup> M. A. H. Vozmediano, M. I. Katsnelson, and F. Guinea, *Physics Reports* **496**, 109 (2010).
  - <sup>12</sup> N. Levy, S. A. Burke, K. L. Meaker, M. Panlasigui, A. Zettl, F. Guinea, A. H. Castro Neto, and M. F. Crommie, *Science* **329**, 544 (2010).
  - <sup>13</sup> C. Lee, X. Wei, J. W. Kysar, and J. Hone, *Science* **321**, 385 (2008).
  - <sup>14</sup> R. Grantab, V. B. Shenoy, and R. S. Ruoff, *Science* **330**, 946 (2010).
  - <sup>15</sup> C. A. Marianetti and H. G. Yevick, *Phys. Rev. Lett.* **105**, 245502 (2010).
  - <sup>16</sup> S.-H. Lee, H.-J. Chung, J. Heo, H. Yang, J. Shin, U.-I. Chung, and S. Seo, *ACS Nano* **5**, 2964 (2011).
  - <sup>17</sup> P. Giannozzi, S. Baroni, N. Bonini, M. Calandra, R. Car, C. Cavazzoni, D. Ceresoli, G. L. Chiarotti, M. Cococcioni, I. Dabo, et al., *J. Phys.: Condens. Matter* **21**, 395502 (2009).
  - <sup>18</sup> N. Troullier and J. L. Martins, *Phys. Rev. B* **43**, 1993 (1991).
  - <sup>19</sup> J. P. Perdew and A. Zunger, *Phys. Rev. B* **23**, 5048 (1981).
  - <sup>20</sup> S. Baroni, S. de Gironcoli, A. Dal Corso, and P. Giannozzi, *Rev. Mod. Phys.* **73**, 515 (2001).
  - <sup>21</sup> K.-P. Bohnen, R. Heid, and C. T. Chan, *J. Phys.: Condens. Matter* **21**, 084206 (2009).
  - <sup>22</sup> G. Savini, A. C. Ferrari, and F. Giustino, *Phys. Rev. Lett.* **105**, 037002 (2010).
  - <sup>23</sup> G. G. Samsonidze, E. B. Barros, R. Saito, J. Jiang, G. Dresselhaus, and M. S. Dresselhaus, *Phys. Rev. B* **75**, 155420 (2007).
  - <sup>24</sup> S. Piscanec, M. Lazzeri, F. Mauri, A. C. Ferrari, and J. Robertson, *Phys. Rev. Lett.* **93**, 185503 (2004).
  - <sup>25</sup> D. M. Clatterbuck, C. R. Krenn, M. L. Cohen, and J. W. Morris, Jr., *Phys. Rev. Lett.* **91**, 135501 (2003).
  - <sup>26</sup> M. Lazzeri, C. Attaccalite, L. Wirtz, and F. Mauri, *Phys. Rev. B* **78**, 081406 (2008).
  - <sup>27</sup> W. Kohn, *Phys. Rev. Lett.* **2**, 393 (1959).
  - <sup>28</sup> F. Liu, P. Ming, and J. Li, *Phys. Rev. B* **76**, 064120 (2007).
  - <sup>29</sup> M. O. Goerbig, J.-N. Fuchs, G. Montambaux, and F. Piéchon, *Phys. Rev. B* **78**, 045415 (2008).
  - <sup>30</sup> K. S. Novoselov, *Rev. Mod. Phys.* **83**, 837 (2011).
  - <sup>31</sup> C. Si, W. Duan, Z. Liu and F. Liu, *Phys. Rev. Lett.* **109**, 226802 (2012).
  - <sup>32</sup> S. Woo and Y.-W. Son, *Bull. Am. Phys. Soc.* **57**, X11.00005 (2012) [<http://meeting.aps.org/link/BAPS.2012.MAR.X11.5>]